

Neutral and Ionic Supramolecular Structures of Unsaturated Dicarboxylic Acids and Acridine: Significance of Molecular Geometry and Proton Transfer

Xuefeng Mei^[a] and Christian Wolf^{*,[a]}

Keywords: Crystal engineering / Supramolecular synthon / X-ray diffraction / Dicarboxylic acid / Acridine

Six supramolecular structures exhibiting distinct architectures have been prepared from acridine and different dicarboxylic acids. The co-crystallization of acridine (**1**) and configurational isomers of dicarboxylic acids such as *cis,trans*-muconic (**a**) and *trans,trans*-muconic acid (**b**), or fumaric (**c**) and maleic acid (**d**) provided strikingly different packing motifs and properties. The supramolecular structures have been rationalized based on the molecular geometry and the constituent synthons. Co-crystallization of acridine and **b**, **c**, or terephthalic acid (**e**) gave neutral assemblies stabilized by the O–H...N hydrogen-bond synthon **I**. Acridine was found to undergo proton transfer with **a**, **d**, and acetylenedicarboxylic acid (**f**) to form ionic supramolecular structures exhibiting synthon **II**, i.e. charge-assisted carboxylate-acridinium O[−]...H–N⁺-hydrogen bonding. The packing mode of **1⁺a[−]** has been inferred from the corresponding acridine-isophthalic acid analog based on the superimposable structure of the ac-

ids and the common charge-assisted hydrogen bonding motif. Acetylenedicarboxylic and *cis,trans*-muconic acid favor the formation of antiparallel acridinium π -stacks stabilized by alternating hydrogen bonds with two infinite anionic chains of dicarboxylic acids that also undergo head-to-tail hydrogen bonding. Because of their different structure and geometry, **b**, **c**, **d**, and **e** form less uniform packing arrangements with **1**. Fumaric and *trans,trans*-muconic acid afford 2:1 neutral co-crystals with parallel acridine rings that are stabilized by π - π -interactions, whereas terephthalic acid favors association of antiparallel acridine dimers to adopt a different one-dimensional network. By contrast, **d** undergoes intramolecular hydrogen bonding which leaves only one carboxyl group available to form a 1:1 ionic supramolecular structure with **1**.

(© Wiley-VCH Verlag GmbH & Co. KGaA, 69451 Weinheim, Germany, 2004)

Introduction

The chemical and physical properties of organic materials depend on the structure and the spatial arrangement of the constituent supramolecular synthons. Crystal engineering is aimed at the prediction of the structure and properties of supramolecular assemblies based on the functionality and geometry of the molecular building blocks.^[1] The design of predictable solid-state assemblies from organic and inorganic compounds exhibiting a structurally diverse but reasonably understood coordination chemistry has become a successful strategy in supramolecular chemistry.^[2] However, crystal engineering of purely organic solids mainly relies on less predictable weak interactions including hydrogen bonding, dipole-dipole interactions, and π -stacking forces.^[3] In analogy to traditional synthetic chemistry, which produces new compounds through covalent bond formation, the preparation of supramolecular co-crystalline materials is based on the complex synergism of non-covalent forces, molecular shape, conformational flexibility, and stoichiometry of complementary molecules.^[4] In addition to the formation of supramolecular assemblies exhibiting unique

properties, e.g. nonlinear optics,^[5] the careful design of two-component molecular crystals has led to the development of powerful template-assisted solid-state reactions.^[6] The unique orientational control of organic molecules in the solid state affords distinguished topochemical and stereochemical selectivities in solvent-free organic transformations.^[7] We therefore decided to employ acridine and dicarboxylic acids exhibiting different geometries in co-crystallization experiments to investigate the effect of molecular geometry and intermolecular interactions on the supramolecular structure.

Results and Discussion

According to solid state interactions observed between aliphatic and aromatic acids and pyridines,^[8] synthons **I** and **II** can be expected to direct the supramolecular organization of complexes consisting of carboxylic acids and acridine (Figure 1). The acid...acridine hydrogen bond in **I**

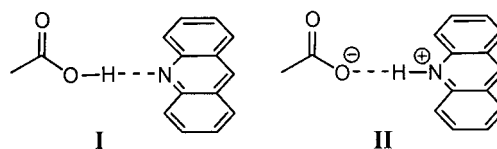


Figure 1. Supramolecular synthons **I** and **II**

^[a] Department of Chemistry, Georgetown University, Washington, DC 20057, USA
Fax: (internat.) + 1-202-687-6209
E-mail: cw27@georgetown.edu

would result in the formation of neutral co-crystals, whereas the charge-assisted hydrogen bond in **II** would afford ionic supramolecular structures.

Recently, co-crystals of acridine and isophthalic or 2,2'-biphenyldicarboxylic acid stabilized by π -stacking and hydrogen bonding have been reported.^[9] In both structures, antiparallel acridinium molecules undergo π -stacking stabilized by anionic chains of dicarboxylic acids. The infinite acid chains were found to be stabilized by strong OH...O bonds and through hydrogen bonding between the carboxylate groups and the acridinium moieties. A closer look at the structure of isophthalic and 2,2'-biphenyldicarboxylic acid suggested that they favor the same packing motif in co-crystals with acridine because of striking similarities in their geometry, intramolecular distance between the carboxylic acid groups, and tendency to form ionic assemblies. We concluded that a dicarboxylic acid such as *cis,trans*-muconic acid exhibiting a nearly superimposable structure is likely to form the same packing arrangement with acridine if charge-assisted interactions **II** were present (Figure 2).

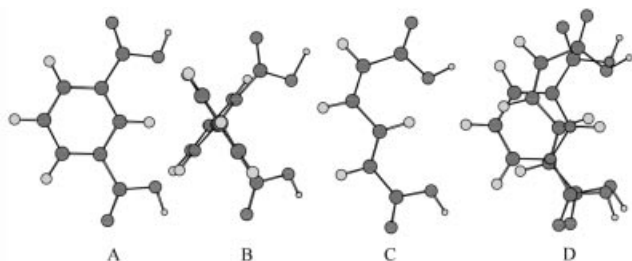


Figure 2. Structures of (A) isophthalic acid, (B) 2,2'-biphenyldicarboxylic acid, (C) *cis,trans*-muconic acid, and superimposed structures of isophthalic and (D) *cis,trans*-muconic acid

We assumed that the supramolecular structure of organic solids prepared from acridine and dicarboxylic acids might also afford other packing arrangements depending on the acid geometry, molecular stoichiometry, and prevailing synthon. We therefore employed *cis,trans*-muconic acid (**a**) *trans,trans*-muconic acid (**b**) fumaric acid (**c**) maleic acid (**d**)

terephthalic acid (**e**) and acetylenedicarboxylic acid (**f**) in co-crystallization experiments with acridine (**1**) (Figure 3).

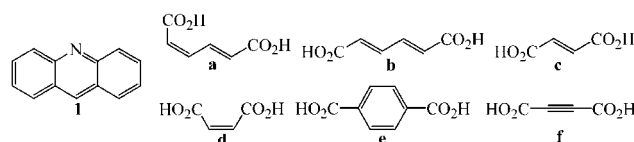
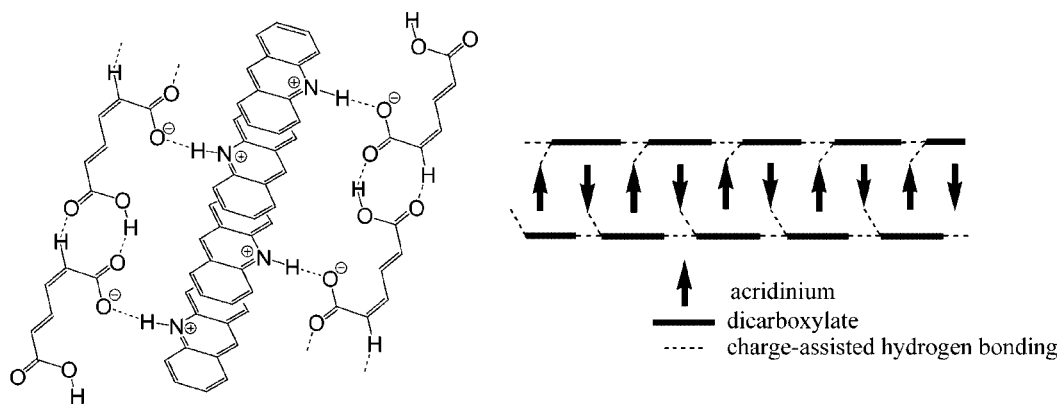


Figure 3. Structures of building blocks **1** and **a–f**

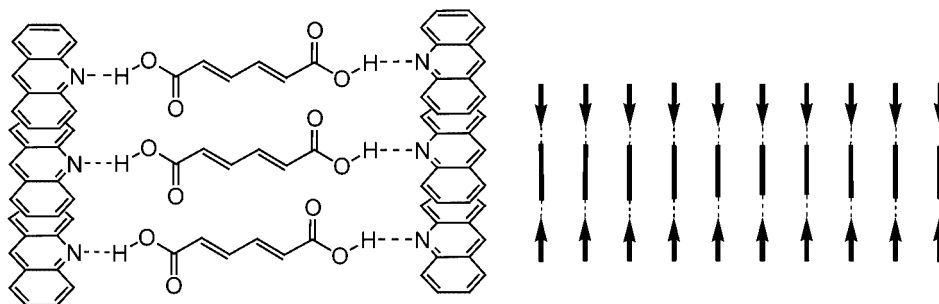
Because of the structural similarity to isophthalic and 2,2'-biphenyldicarboxylic acid, one would expect *cis,trans*-muconic acid to undergo similar interactions with acridine in solution prior to nucleation and crystallization. It seems reasonable to assume that the structure of a supramolecular assembly of **1** and **a** is a result of a distinct recognition mechanism operative in a supersaturated solution prior to crystallization. The (*E,Z*)-geometry of **a** and the intramolecular distance between the two carboxylic acid groups of **a** should therefore favor formation of ionic aggregates consisting of π -stacks of antiparallel acridinium rings bridged by bidentate dicarboxylic acids (Scheme 1). The recognition pattern would then be replicated to a corresponding packing motif during co-crystallization.

Because the supramolecular organization, i.e. formation of a neutral (synthon **I**) or ionic (synthon **II**) structure, of carboxylic acid-pyridine complexes has been found to depend on the structure of the acid used,^[8] we expected that the employment of dicarboxylic acids with different geometry may also result in neutral co-crystals. For example, **b** has a significantly lower acidity than **a** and was expected to favor bridging between π -stacks of parallel acridine units to form a co-crystalline structure based on synthon **I** (Scheme 2). Accordingly, **a** and **b** would afford strikingly different aggregates in solution that consequently result in the formation of distinct ionic or neutral solid-state structures.

We were able to grow a triclinic co-crystal of **1**⁺·**a**[−] belonging to the space group $P\bar{1}$ through careful evaporation



Scheme 1. Proposed molecular recognition between *cis,trans*-muconic acid and acridine (left) and schematic illustration of the corresponding packing motif in an ionic supramolecular structure of antiparallel acridinium rings and equimolar amounts of infinite isophthalic or 2,2'-biphenyldicarboxylic acid anions bridging the aromatic π -stack on both sides (right)



Scheme 2. Predicted interaction between *trans,trans*-muconic acid and acridine (left) and schematic illustration of the corresponding packing motif in co-crystals of parallel acridine rings and dicarboxylic acids bridging between aromatic π -stacks (right)

of an EtOH/H₂O (5:1) solution. The structure of $1^+ \cdot a^-$ shows antiparallel acridinium molecules stabilized by π - π interactions and by charge-assisted hydrogen bonding with the carboxylate group attached to the (*Z*)-vinyl moiety of monobasic **a** (Figure 4). The (*E*)-vinyl acid function participates in head-to-tail hydrogen bonding with an adjacent dicarboxylic acid molecule to form anionic polymeric chains of **a** on both sides of the acridinium π -stacks. The distance between the acridinium rings alternates between 3.32 Å and 3.57 Å. The infinite acid chains are stabilized by intermolecular OH \cdots O⁻ (1.75 Å, 163.4°) and CH \cdots O (2.40 Å, 158.2°) bonds. The bond length and angle of the N⁺H \cdots O⁻ bond were determined as 1.69 Å and 175.6°.

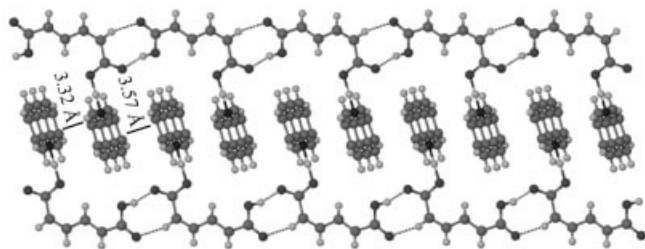


Figure 4. Crystal structure of $1^+ \cdot a^-$ exhibiting antiparallel acridinium ions and polymeric carboxylate chains

The crystal lattice of $1^+ \cdot a^-$ is in excellent agreement with the packing motif depicted in Scheme 1 and resembles the ionic structure and synthon **II** obtained with superimposable isophthalic and 2,2'-biphenyldicarboxylic acid. The space-filling model shows the one-dimensional network formed by π -stacked antiparallel acridine rings (Figure 5).

Slow evaporation of a MeOH/H₂O (1:1) solution gave neutral monoclinic co-crystals of **1·b** belonging to the $P2_1/c$ space group. Interestingly, the structure of **1·b** follows the packing motif shown in Scheme 2. The crystal lattice is stabilized by hydrogen bonding and π -stacking between offset acridines (Figure 6). The OH \cdots N bond length and angle were determined as 1.85 Å and 170°. The acid molecules are oriented almost perpendicular to the acridine rings and form a planar network of weak hydrogen bonds between carboxylic oxygens and two vinylic hydrogens of adjacent molecules. Multiple hydrogen bonding between **b** thus enforces the offset stacking of the acridine rings. The length and angle of these CH \cdots O bonds were found to be 2.46 Å

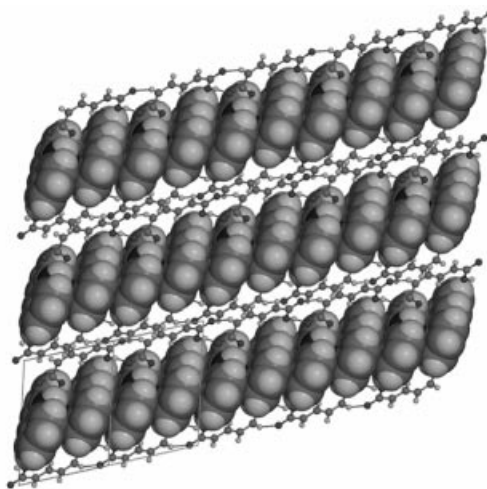


Figure 5. Projection of the one-dimensional network of $1^+ \cdot a^-$ consisting of antiparallel acridinium (space-filling model) and colinear polymers of the dicarboxylate molecules

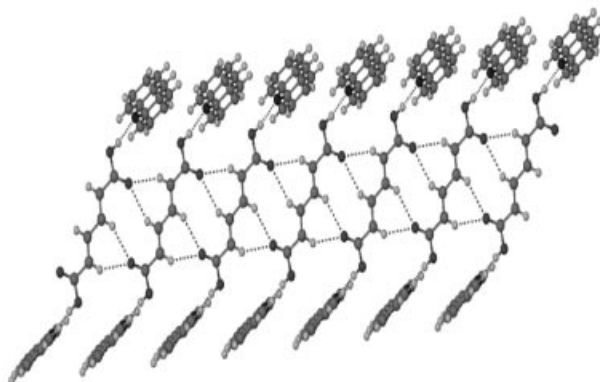
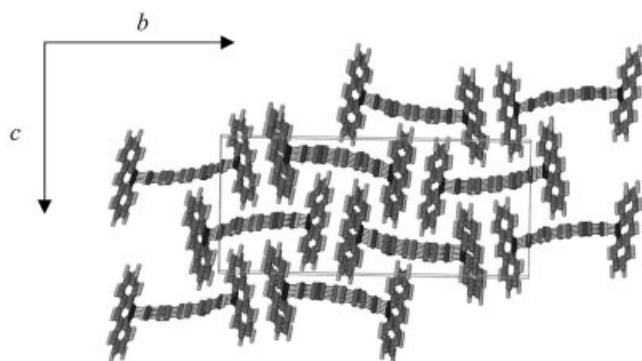


Figure 6. Crystal structure of **1·b** exhibiting parallel acridines

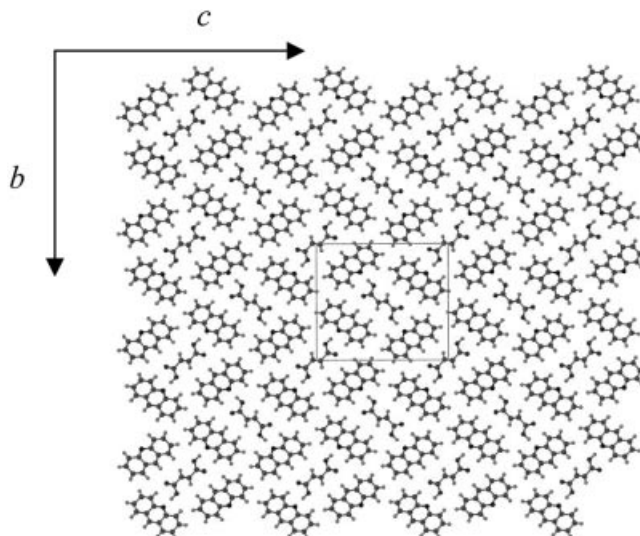
(149°) and 2.52 Å (148°), respectively.^[10] The crystal structure thus displays one-dimensional networks consisting of a 2:1 ratio of parallel acridines and coplanar dicarboxylic acids **b** (Figure 7).

Our results clearly show that the crystallization of **1** and configurational isomers **a** and **b** results in the formation of supramolecular structures $1^+ \cdot a^-$ and **1·b**, respectively, exhibiting strikingly different molecular orientations, stoichiometry, and synthons. In order to explore the significance of the molecular geometry of the dicarboxylic acids on the

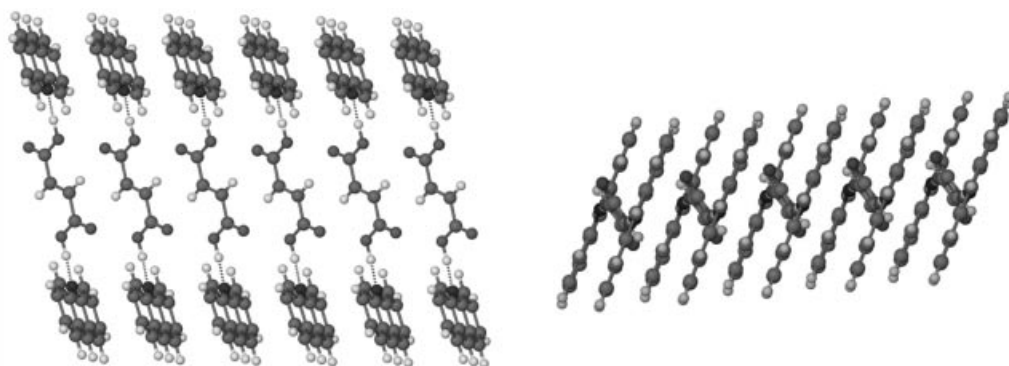
Figure 7. Projection of the one-dimensional network of **1·b**

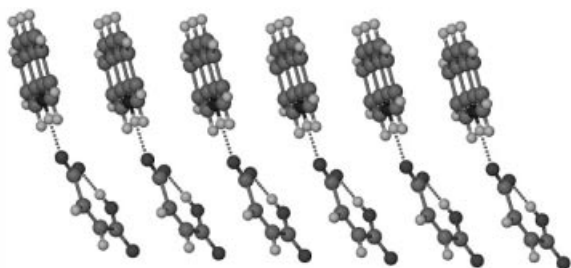
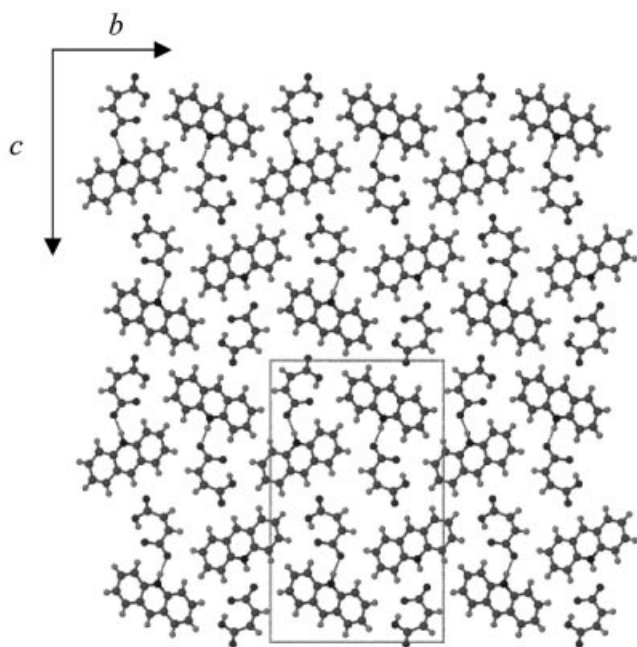
supramolecular structure and the generality of the packing motif depicted in Schemes 1 and 2, we decided to grow single co-crystals of **1** and dicarboxylic acids **c–f**.

We obtained **1·c** by isothermal evaporation of an acetonitrile solution as monoclinic crystals (space group $P2_1/c$), Figure 8 and Figure 9. The co-crystal consists of two equivalents of parallel **1** and one equivalent of **c** bridging between two acridine π -stacks. The O–H \cdots N hydrogen bond length and angle were determined as 1.61 Å and 176°. It should be noted that the dicarboxylic acids are arranged at a 64° angle to the acridine rings. Accordingly, they are not coplanar and cannot undergo intermolecular CH \cdots O hydrogen bonding as was observed for **1·b**. The herring bone packing of **1·c** is stabilized by two different face-to-face-interactions forming acridine and fumaric acid π -stacks. The distance between the cofacial acridine rings is 3.47 Å. It is noteworthy that the fumaric acid molecules are only 3.39 Å apart. The close proximity and orientational control of cofacial fumaric acid molecules in a well-defined supramolecular structure such as **1·c** may provide a quite promising venue for the formation of new covalent bonds through solid-state reactions. Acridine and unsaturated acids such as **c** may therefore be used as complimentary supramolecular building blocks to construct new organic materials or to form new covalent bonds with high topochemical and stereochemical selectivities inherent to solid-state chemistry.

Figure 9. Herring bone packing of **1·c** along the *a* axis

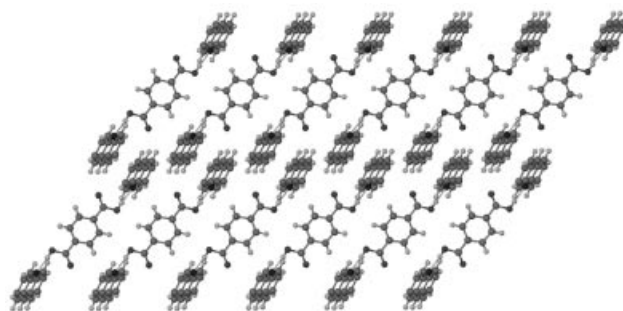
Isothermal ethanol evaporation using an equimolar solution of acridine and maleic acid gave monoclinic **1⁺·d[–]** belonging to the $P2_1/n$ space group. Because of the short distance between the carboxylic acid functions in maleic acid and its known preference for intramolecular hydrogen bonding, **d** and **1** afford a unique supramolecular architecture. In analogy to the assemblies obtained with acridine and isomeric acids **a** and **b**, we expected that **c** and **d** would also form strikingly different supramolecular structures. Indeed, the structure of **1⁺·d[–]** shows parallel acridinium rings stabilized by π – π -interactions and hydrogen bonding to maleate molecules, which undergo intramolecular OH \cdots O $^-$ hydrogen bonding (1.62 Å, 177°) and therefore do not bridge between two stacks of parallel acridinium rings (Figure 10 and Figure 11). The distance between the acridinium rings is 3.45 Å and the closest contact between the maleate double bonds is 3.57 Å. The N $^+$ H \cdots O $^-$ bond length was determined as 1.77 Å (172°).

Figure 8. Crystal structure of **1·c**. Projection along the *b* axis showing the formation of one-dimensional networks stabilized by hydrogen bonding and π – π -interactions (left) and view of the fumaric acid and acridine π -stacking (right)

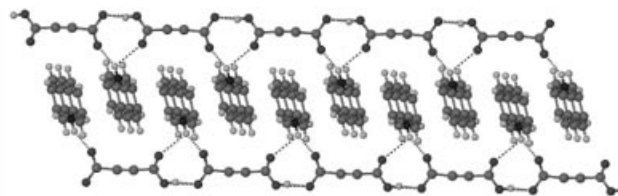
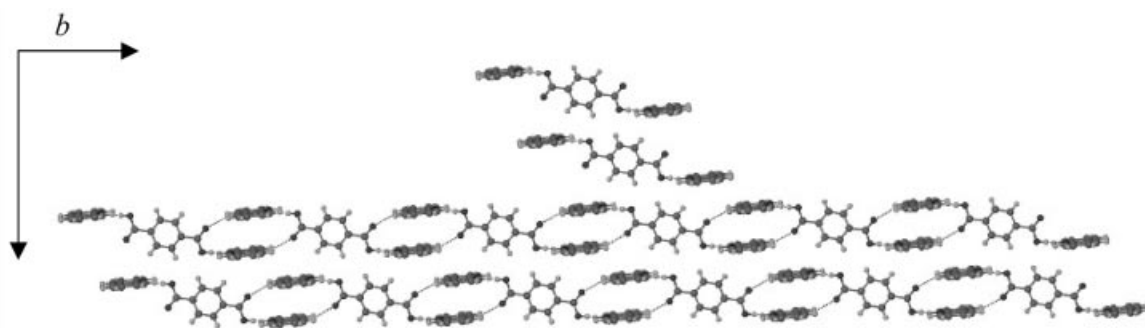
Figure 10. Crystal structure of $1^+\cdot d^-$ Figure 11. Projection of the packing motif of $1^+\cdot d^-$ along the a axis

Although terephthalic acid affords a similar distance between the two carboxylic acid groups as *cis,trans*-muconic acid, the phenyl spacer can be expected to impede hydrogen bonding directed to the same side of the diacid supramolecular synthon as observed with $1^+\cdot a^-$. We therefore expected **e** to favor a crystal lattice similar to **1·b** or **1·c**. Co-crystallization of **1·e** from DMF afforded monoclinic crystals belonging to the $P2_1/n$ space group (Figure 12). Inter-

estingly, the neutral supramolecular structure of **1·e** is somewhat similar to that of **1·b** and **1·c** since the dicarboxylic acid molecules do not undergo proton transfer with **1** and participate in hydrogen bonding with two acridine molecules affording synthon **I**. A closer look at the crystal structure reveals that arrays of parallel acridine molecules are intertwined to form pairs of antiparallel acridine dimers stabilized by $\pi-\pi$ -interactions (Figure 13). The dimers are bridged by $OH\cdots N$ (1.76 Å, 176°) and $CH\cdots O$ (2.40 Å, 151°) hydrogen bonds. The distance between the bridged antiparallel acridines is 3.39 Å. Although the stoichiometry and acridine bridging motif of **1·e** resembles that of **1·c** and **1·b** the association of antiparallel acridine dimers connected by terephthalic acid linkers results in a new one-dimensional network.

Figure 12. Crystal structure of **1·e**

Careful solvent evaporation of an ethanol solution of acridine and acetylenedicarboxylic acid gave triclinic assembly $1^+\cdot f^-$ belonging to the $P\bar{1}$ space group (Figure 14). The structure of dicarboxylic acid **f** should, in principle, be compatible with both molecular recognition models discussed above. The intramolecular distance between the acid

Figure 14. Crystal structure of $1^+\cdot f^-$ showing hydrogen bonds and $\pi-\pi$ -interactionsFigure 13. Projection of **1·e** showing the chains formed by bridging of acridine dimers through $OH\cdots N$ and $CH\cdots O$ hydrogen bonds with terephthalic acid molecules

functions of **f** is similar to **a** and **e**. However, the acetylene spacer of **f** does not impede unidirectional hydrogen bonding which was found to be indispensable for bridging within acridine π -stacks as was observed in the structure of $1^+ \cdot a^-$ (Scheme 1). This and the proton transfer reaction with acridine is an important structural difference to dicarboxylic acid **e** exhibiting a bulky benzene group between its acid moieties which favors bridging between acridine π -stacks (Scheme 2). Crystallographic analysis of $1^+ \cdot f^-$ revealed an ionic supramolecular assembly displaying a 1:1 stoichiometry as was observed for $1^+ \cdot a^-$ (Figure 15). The linear acetylene dicarboxylate molecules undergo head-to-tail hydrogen bonding to form infinite anionic chains that participate in alternating hydrogen bonding with antiparallel acridinium ions. The proton transfer from one acid moiety to the acridyl nitrogen results in a strong $N^+H \cdots O^-$ hydrogen bond (1.91 Å, 154°) and a weak $N^+H \cdots O'$ bond (2.52 Å, 113°) to the adjacent carboxylic acid. The length and angle of the $OH \cdots O^-$ hydrogen bonding were determined as 1.63 Å and 168°. The distance between the acridinium rings was found to be 3.53 Å.

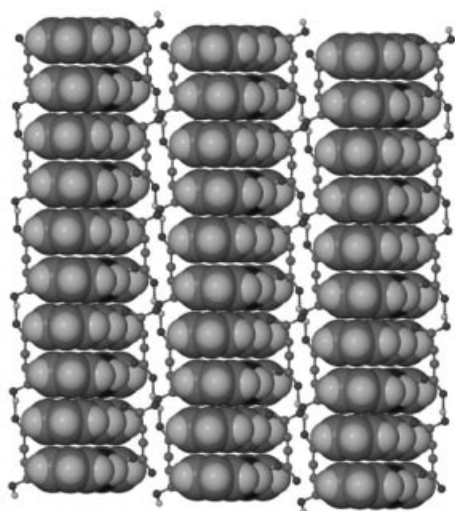


Figure 15. Projection of antiparallel acridiniums (space-filling model) and polymers of acetylene dicarboxylate in $1^+ \cdot f^-$.

The occurrence of proton transfer between carboxylic acids and pyridines in the solid state has been correlated to a difference in pKa values between the constituent pyridinium ion and the carboxylic acid.^[11] Accordingly, ionic complexes are to be expected for $\Delta pK_a > 3.75$, whereas neutral

co-crystals would form for $\Delta pK_a < 3.75$. A comparison of the acidity of carboxylic acids **a–f** and acridinium $1-H^+$ shows that based on the first pKa value *cis,trans*-muconic, maleic and acetylenedicarboxylic acid fulfil this requirement, whereas *trans,trans*-muconic, fumaric, and terephthalic acids should form neutral complexes in the solid state (Table 1). Although our experimental results are in agreement with this empirical rule a rationalization of the preference for synthon **I** or **II** based on ΔpK_a data is difficult and does not explain why both acid functions of *cis,trans*-muconic, maleic and acetylenedicarboxylic acid undergo proton transfer since pKa values for the second acid function of **a**, **d** and **f** are significantly higher. It should be noted that proton transfer between aromatic heterocycles and carboxylic acids has been found to occur in solution or during crystallization.^[8a] The prediction of ionic or neutral hydrogen bonding based on pKa values determined in solution or in solution NMR studies is therefore limited.^[8b]

Table 1. Acidity of acridinium $1-H^+$ and dicarboxylic acids **a** to **f**

Entry	pKa ₁	pKa ₂	$\Delta pK_{a1}^{[a]}$	$\Delta pK_{a2}^{[a]}$	Hydrogen bonding
a	1.90	4.79	3.86	0.97	synthon II
b	2.70	4.66	3.06	1.10	synthon I
c	3.03	4.44	2.73	1.32	synthon I
d	1.97	6.24	3.79	−0.48	synthon II
e	3.51	4.82	2.25	0.94	synthon I
f	1.75	4.40	4.01	1.36	synthon II

^[a] The pKa value of $1-H^+$ is 5.76.

The distinctive hydrogen bonding pattern and architecture of the co-crystals obtained from acridine and acids **a–f** result in strikingly different properties (Table 2). The neutral co-crystals have significantly higher melting points than the ionic assemblies. The melting points of triclinic $1^+ \cdot a^-$ and $1^+ \cdot f^-$ belonging to the $P\bar{1}$ space group were determined as 136 °C and 133 °C, respectively. The monoclinic co-crystals obtained with acids **b** and **c** afford a $P2_1/c$ space group and melt at significantly higher temperatures, 199 °C and 191 °C, respectively, whereas monoclinic $1^+ \cdot d^-$ and $1^+ \cdot e^-$ belong to the $P2_1/n$ space group and have a melting point of 113 °C or 259 °C. All supramolecular architectures have higher melting points than acridine, which can be attributed to the formation of synthons **I** and **II**, but lower melting points than the individual dicarboxylic acids.^[12]

Table 2. Crystallographic data for supramolecular assemblies $1^+ \cdot a^-$ to $1^+ \cdot f^-$

Parameter	$1^+ \cdot a^-$	1·b	1·c	$1^+ \cdot d^-$	1·e	$1^+ \cdot f^-$
Crystal system	triclinic	monoclinic	monoclinic	monoclinic	monoclinic	triclinic
Space group	$P\bar{1}$	$P2_1/c$	$P2_1/c$	$P2_1/n$	$P2_1/n$	$P\bar{1}$
Z	2	4	4	4	4	2
$\rho_{\text{calcd.}}$ [g/cm ³]	1.365	1.304	1.395	1.431	1.307	1.424
m.p. [°C]	136	199	191	113	259	133

Conclusion

Distinct supramolecular assemblies constructed from **1** and dicarboxylic acids **a–f** of varying acidity, size, and geometry have been prepared. Employing *cis,trans*-muconic and *trans,trans*-muconic or maleic and fumaric acid in co-crystallization experiments with acridine, we were able to show that molecular isomerism can be systematically transformed into distinct supramolecular architectures exhibiting either neutral or ionic structures with strikingly different properties. The supramolecular structures were rationalized based on acid geometry and synthon formation.

Superimposable isophthalic, 2,2'-biphenyldicarboxylic, and *cis,trans*-muconic acid, undergo charge-assisted hydrogen bonding to afford acridinium-dicarboxylated assemblies with a common ionic supramolecular structure. Acetylenedicarboxylic and *cis,trans*-muconic acid form ionic assemblies consisting of π -stacks of antiparallel acridinium molecules. The acridinium stacks are stabilized by alternating hydrogen bonds with two infinite dicarboxylate chains exhibiting head-to-tail hydrogen bonding. These structures are composed of one-dimensional networks consisting of equimolar amounts of the complimentary building units. Because of their different structure and geometry, maleic, fumaric, *trans,trans*-muconic, and terephthalic acid are less likely to form polymeric chains along acridinium π -stacks. Employing equimolar amounts of fumaric, *trans,trans*-muconic, and terephthalic acid in crystallization experiments with acridine afforded neutral 2:1 co-crystals exhibiting hydrogen bonding between two acridine rings and one dicarboxylic acid molecule. Fumaric and *trans,trans*-muconic acid afford parallel acridine rings that are stabilized by π - π -interactions, whereas terephthalic acid favors association of antiparallel acridine dimers to adopt a different one-dimensional packing motif. By contrast, maleic acid was found to undergo proton transfer with **1** and intramolecular hydrogen bonding, which leaves only one carboxyl group available to form a 1:1 ionic architecture with acridinium ions.

Experimental Section

Crystal Growth: Equimolar amounts of acridine and acids **a–f** were employed in all crystallization experiments. Co-crystals of **1**⁺·**a**[−] were prepared through slow evaporation of an EtOH/H₂O (5:1) solution containing acridine and *cis,trans*-muconic acid. Using *trans,trans*-muconic acid in MeOH/H₂O (1:1) gave co-crystals of **1**·**b**. Slow evaporation of an acetonitrile solution of fumaric acid and acridine gave **1**·**c**. Co-crystallization of acridine with maleic or acetylenedicarboxylic acid by isothermal ethanol evaporation afforded **1**⁺·**d**[−] or **1**⁺·**f**[−], respectively. Co-crystals of **1**·**e** were obtained by slow crystallization from DMF.

X-ray Single-Crystal Structure Analysis: Single-crystal X-ray diffraction was performed by using a Siemens platform diffractometer with graphite monochromated Mo-K α radiation ($\lambda = 0.71073$ Å). Data were integrated with the Siemens SAINT program and corrected for the affects of absorption using SADABS. The structures

were solved by direct methods and refined with full-matrix least-squares analysis using SHELX-97-2 software. Non-hydrogen atoms were refined with anisotropic displacement parameters and all hydrogen atoms were placed in calculated positions and refined with a riding model.

CCDC 239909–239914 contain the supplementary crystallographic data for this paper. These data can be obtained free of charge at www.ccdc.cam.ac.uk/conts/retrieving.html [or from the Cambridge Crystallographic Data Centre, 12 Union Road, Cambridge CB2 1EZ, UK; Fax: +44-1223-336033; E-mail: deposit@ccdc.cam.ac.uk].

Crystal Structure Data for **1⁺·**a**[−]:** Formula C₁₉H₁₅NO₄, $M = 321.32$, crystal dimensions $0.5 \times 0.2 \times 0.2$ mm, triclinic, space group $P\bar{1}$, $a = 8.943(3)$ Å, $b = 9.511(3)$ Å, $c = 11.097(4)$ Å, $\alpha = 67.177(5)^\circ$, $\beta = 87.094(6)^\circ$, $\gamma = 65.098(5)^\circ$, $V = 781.9(5)$ Å³, $Z = 2$, $\rho_{\text{calcd.}} = 1.3646$ g cm^{−3}, $2\theta_{\text{max}} = 56.164^\circ$, $T = 182$ K, 3533 independent reflections ($R_{\text{int}} = 1.90\%$), of which 2698 were above $4\sigma(F)$. $R1 = 0.0403$, $wR2 = 0.1204$ with $I > 2\sigma(I)$, $R_\sigma = 0.0287$, $\text{GooF} = 1.082$, $\Delta\rho_{\text{max}} = 0.31$ e·Å^{−3}, $\Delta\rho_{\text{min}} = -0.27$ e·Å^{−3}.

Crystal Structure Data for **1·**b**:** Formula C₃₂H₂₄N₂O₄, $M = 500.53$, crystal dimensions $0.3 \times 0.1 \times 0.1$ mm, monoclinic, space group $P2_1/c$, $a = 5.7053(7)$ Å, $b = 31.740(4)$ Å, $c = 14.2207(17)$ Å, $\beta = 98.036(2)^\circ$, $V = 2549.9(5)$ Å³, $Z = 4$, $\rho_{\text{calcd.}} = 1.304$ g cm^{−3}, $2\theta_{\text{max}} = 49.38^\circ$, $T = 186(2)$ K, 6065 independent reflections ($R_{\text{int}} = 5.87\%$), of which 2945 were above $4\sigma(F)$. $R1 = 0.0398$, $wR2 = 0.1120$ with $I > 2\sigma(I)$, $R_\sigma = 0.0858$, $\text{GooF} = 0.868$, $\Delta\rho_{\text{max}} = 0.18$ e·Å^{−3}, $\Delta\rho_{\text{min}} = -0.17$ e·Å^{−3}.

Crystal Structure Data for **1·**c**:** Formula C₁₅H₁₁NO₂, $M = 237.25$, crystal dimensions $0.5 \times 0.3 \times 0.3$ mm, monoclinic, space group $P2_1/c$, $a = 3.9922(7)$ Å, $b = 15.823(3)$ Å, $c = 17.892(3)$ Å, $\beta = 88.617(4)^\circ$, $V = 1129.3(3)$ Å³, $Z = 4$, $\rho_{\text{calcd.}} = 1.395$ g cm^{−3}, $2\theta_{\text{max}} = 55.088^\circ$, $T = 184(2)$ K, 2638 independent reflections ($R_{\text{int}} = 4.20\%$), of which 1744 were above $4\sigma(F)$. $R1 = 0.0413$, $wR2 = 0.1024$ with $I > 2\sigma(I)$, $R_\sigma = 0.0443$, $\text{GooF} = 0.994$, $\Delta\rho_{\text{max}} = 0.20$ e·Å^{−3}, $\Delta\rho_{\text{min}} = -0.20$ e·Å^{−3}.

Crystal Structure Data for **1⁺·**d**[−]:** Formula C₁₇H₁₃NO₄, $M = 295.28$, Crystal dimensions $0.5 \times 0.1 \times 0.05$ mm, monoclinic, space group $P2_1/n$, $a = 3.950(2)$ Å, $b = 14.622(6)$ Å, $c = 23.733(9)$ Å, $\beta = 90.89(9)^\circ$, $V = 1370.4$ Å³, $Z = 4$, $\rho_{\text{calcd.}} = 1.4310$ g cm^{−3}, $2\theta_{\text{max}} = 50^\circ$, $T = 186(2)$ K, 2418 independent reflections ($R_{\text{int}} = 5.28\%$), of which 1689 were above $4\sigma(F)$. $R1 = 0.047$, $wR2 = 0.127$ with $I > 2\sigma(I)$, $R_\sigma = 0.053$, $\text{GooF} = 1.069$, $\Delta\rho_{\text{max}} = 0.18$ e·Å^{−3}, $\Delta\rho_{\text{min}} = -0.25$ e·Å^{−3}.

Crystal Structure Data for **1·**e**:** Formula C₁₇H₁₂NO₂, $M = 262.29$, crystal dimensions $0.5 \times 0.2 \times 0.2$ mm, monoclinic, space group $P2_1/n$, $a = 13.264(2)$ Å, $b = 7.369(1)$ Å, $c = 14.082(1)$ Å, $\beta = 104.45(1)^\circ$, $V = 1332.9(1)$ Å³, $Z = 4$, $\rho_{\text{calcd.}} = 1.3069$ g cm^{−3}, $2\theta_{\text{max}} = 56^\circ$, $T = 186(2)$ K, 3134 independent reflections ($R_{\text{int}} = 5.34\%$), of which 1618 were above $4\sigma(F)$. $R1 = 0.0458$, $wR2 = 0.1199$ with $I > 2\sigma(I)$, $R_\sigma = 0.0601$, $\text{GooF} = 0.949$, $\Delta\rho_{\text{max}} = 0.17$ e·Å^{−3}, $\Delta\rho_{\text{min}} = -0.22$ e·Å^{−3}.

Crystal Structure Data for **1⁺·**f**[−]:** Formula C₁₇H₁₁NO₄, $M = 293.27$, crystal dimensions $0.5 \times 0.2 \times 0.2$ mm, triclinic, space group $P\bar{1}$, $a = 7.845(2)$ Å, $b = 8.902(2)$ Å, $c = 10.589(3)$ Å, $\alpha = 73.626(4)^\circ$, $\beta = 88.617(4)^\circ$, $\gamma = 74.920(4)^\circ$, $V = 684.1(3)$ Å³, $Z = 2$, $\rho_{\text{calcd.}} = 1.4237$ g cm^{−3}, $2\theta_{\text{max}} = 54.82^\circ$, $T = 185$ K, 2385 independent reflections ($R_{\text{int}} = 3.04\%$), of which 1714 were above $4\sigma(F)$. $R1 = 0.0545$, $wR2 = 0.1287$ with $I > 2\sigma(I)$, $R_\sigma = 0.0491$, $\text{GooF} = 1.078$, $\Delta\rho_{\text{max}} = 0.21$ e·Å^{−3}, $\Delta\rho_{\text{min}} = -0.21$ e·Å^{−3}.

- [1] [1a] G. R. Desiraju, *Crystal engineering: The Design of Organic Solids*, Elsevier, New York, **1989**. [1b] T. L. Hennigar, D. C. MacQuarrie, P. Losier, R. D. Rogers, M. J. Zaworotko, *Angew. Chem. Int. Ed. Engl.* **1997**, *36*, 972–973. [1c] J. A. Swift, A. M. Pivovarov, A. M. Reynolds, M. D. Ward, *J. Am. Chem. Soc.* **1998**, *120*, 5887–5894. [1d] B. Moulton, M. J. Zaworotko, *Chem. Rev.* **2001**, *101*, 1629–1658. [1e] J. A. McMahon, M. J. Zaworotko, J. F. Remenar, *Chem. Commun.* **2004**, 278–279. [1f] J. F. Remenar, S. L. Morissette, M. L. Peterson, B. Moulton, J. M. MacPhee, H. R. Guzman, O. Almarsson, *J. Am. Chem. Soc.* **2003**, *125*, 8456–8457.
- [2] [2a] A. H. Mahmoudkhani, V. Langer, *Cryst. Growth Des.* **2002**, *2*, 21–25. [2b] H. Abourahma, B. Moulton, V. Kravtsov, M. J. Zaworotko, *J. Am. Chem. Soc.* **2002**, *124*, 9990–9991. [2c] B. Zimmer, V. Bulach, M. W. Hosseini, A. De Cian, N. Kyritsakas, *Eur. J. Inorg. Chem.* **2002**, 3079–3082. [2d] R. P. Doyle, P. E. Kruger, B. Moubarak, K. S. Murray, M. Nieuwenhuyzen, *Dalton Trans.* **2003**, 4230–4237. [2e] C.-Y. Su, A. M. Goforth, M. D. Smith, H.-C. zur Loye, *Inorg. Chem.* **2003**, *42*, 5685–5692.
- [3] [3a] J. J. Kane, R.-F. Liao, J. W. Lauher, F. W. Fowler, *J. Am. Chem. Soc.* **1995**, *117*, 12003–12004. [3b] H. Koshima, T. Nakagawa, T. Matsuura, H. Miyamoto, F. Toda, *J. Org. Chem.* **1997**, *62*, 6322–6325. [3c] E. Batchelor, J. Klinowski, W. Jones, *J. Mater. Chem.* **2000**, *10*, 839–848. [3d] M. Gdaniec, W. Jankowski, M. J. Milewska, T. Polonski, *Angew. Chem. Int. Ed.* **2003**, *42*, 3903–3906. [3e] B. Olenik, T. Smolka, R. Boese, R. Sustmann, *Cryst. Growth Des.* **2003**, *3*, 183–188. [3f] A. Crihfield, J. Hartwell, D. Phelps, R. B. Walsh, J. L. Harris, J. F. Payne, W. T. Pennington, T. W. Hanks, *Cryst. Growth Des.* **2003**, *3*, 313–320.
- [4] C. B. Aakeroy, A. M. Beatty, B. A. Helfrich, *J. Am. Chem. Soc.* **2002**, *124*, 14425–14432.
- [5] [5a] S. R. Marder, J. W. Perry, W. P. Schaefer, *Science* **1989**, *245*, 626–628. [5b] S. R. Marder, J. W. Perry, B. G. Tiemann, *Chem. Mater.* **1990**, *2*, 685–690. [5c] S. R. Marder, J. W. Perry, B. G. Tiemann, *Organometallics* **1991**, *10*, 1896–1901. [5d] S. R. Marder, J. W. Perry, C. P. Yakymyshyn, *Chem. Mater.* **1994**, *6*, 1137–1147. [5e] H. Kagawa, M. Sagawa, T. Hamada, A. Kakuta, *Chem. Mater.* **1996**, *8*, 2622–2627. [5f] S. Lochran, R. T. Bailey, F. R. Cruickshank, D. Pugh, J. N. Sherwood, G. S. Simpson, P. J. Langley, J. D. Wallis, *J. Phys. Chem. B* **2000**, *104*, 6710–6716. [5g] T. Pal, T. Kar, G. Bocelli, L. Rigi, *Cryst. Growth Des.* **2003**, *3*, 13–16.
- [6] [6a] H. Koshima, K. Ding, Y. Chisaka, T. Matsuura, *J. Am. Chem. Soc.* **1996**, *118*, 12059–12065. [6b] H. Koshima, T. Nakagawa, T. Matsuura, *Tetrahedron Lett.* **1997**, *38*, 6063–6066. [6c] H. Koshima, K. Ding, Y. Chisaka, T. Matsuura, I. Miyahara, K. Hirotsu, *J. Am. Chem. Soc.* **1997**, *119*, 10317–10324. [6d] G. W. Coates, A. R. Dunn, L. M. Henling, J. W. Ziller, E. B. Lobkovsky, R. H. Grubbs, *J. Am. Chem. Soc.* **1998**, *120*, 3641–3649. [6e] A. Matsumoto, T. Odani, M. Chikada, K. Sada, M. Miyata, *J. Am. Chem. Soc.* **1999**, *121*, 11122–11129. [6f] Y. Ito, H. Hosomi, S. Ohba, *Tetrahedron* **2000**, *56*, 6833–6844. [6g] A. Matsumoto, S. Nagahama, T. Odani, *J. Am. Chem. Soc.* **2000**, *122*, 9109–9119. [6h] A. Matsumoto, K. Sada, K. Tashiro, M. Miyata, T. Tsubouchi, T. Tanaka, T. Odani, S. Nagahama, T. Tanaka, K. Inoue, S. Saragai, S. Nakamoto, *Angew. Chem. Int. Ed.* **2002**, *41*, 2502–2505. [6i] X. Ouyang, F. W. Fowler, J. W. Lauher, *J. Am. Chem. Soc.* **2003**, *125*, 12400–12401. [6j] X. Gao, T. Friscic, L. R. MacGillivray, *Angew. Chem. Int. Ed.* **2004**, *43*, 232–236.
- [7] [7a] K. Tashiro, T. Kamae, M. Kobayashi, A. Matsumoto, K. Yokoi, S. Aoki, *Macromolecules* **1999**, *32*, 2449–2454. [7b] A. Matsumoto, K. Katayama, T. Odani, K. Oka, K. Tashiro, S. Saragai, S. Nakamoto, *Macromolecules* **2000**, *33*, 7786–7792. [7c] T. Tanaka, A. Matsumoto, *J. Am. Chem. Soc.* **2002**, *124*, 9676–9677. [7d] A. Matsumoto, S. Oshita, D. Fujioka, *J. Am. Chem. Soc.* **2002**, *124*, 13749–13756.
- [8] [8a] I. S. Lee, D. M. Shin, Y. K. Chung, *Cryst. Growth Des.* **2003**, *3*, 521–529. [8b] B. R. Bhogala, A. Nangia, *Cryst. Growth Des.* **2003**, *3*, 547–554.
- [9] [9a] Z. Shaameri, N. Shan, W. Jones, *Acta Crystallogr., Sect. E* **2001**, *57*, o1075–o1077. [9b] Z. Shaameri, N. Shan, W. Jones, *Acta Crystallogr., Sect. E* **2001**, *57*, o945–o946.
- [10] The combined van der Waals radius of oxygen and hydrogen is 2.73 Å.
- [11] [11a] D. E. Lynch, I. McClenaghan, *Acta Crystallogr., Sect. B* **2001**, *57*, 830–832. [11b] K.-S. Huang, D. Britton, M. C. Etter, S. R. Byrn, *J. Mater. Chem.* **1997**, *7*, 713–720. [11c] P. Vishwehwar, A. Nangia, V. M. Lynch, *J. Org. Chem.* **2002**, *67*, 556–565.
- [12] Melting point ranges [°C]: **1**, 105–110; **a**, 194–195; **b**, 290 (dec.); **c**, 287; **d**, 137–140; **e**, >300; **f**, 180–187.

Received June 3, 2004